

Propagation phenomena in P-wave AVO analysis for transversely isotropic media: A modeling study

Petr Jílek

ABSTRACT

In the analysis of amplitude-variation-with-offset (AVO), used in oil exploration for characterization of hydrocarbon reservoirs, amplitudes are usually corrected for geometrical spreading and radiation pattern and then taken as being proportional to the reflection coefficient for the target horizon. The corrections for propagation phenomena are commonly performed under the assumption of a homogeneous isotropic overburden.

Amplitudes of seismic waves propagating in a single layer with VTI (transversely isotropic with a vertical symmetry axis) symmetry have been previously studied by Tsvankin (1995). Here, I perform numerical modeling of P -wave reflection for an overburden modeled as an isotropic layer above a VTI shale layer, and discuss the influence of the anisotropic overburden on the AVO responses.

An anisotropic overburden causes two major phenomena not present in homogeneous isotropic media: splitting of group and phase velocity vectors, and focusing and defocusing of energy along the wavefront. Without taking into account anisotropy of the overburden in the correction of AVO amplitudes, computed AVO gradients and intercepts may differ significantly from the correct quantities.

Of the factors that can distort AVO amplitudes, anisotropy has only mild influence on P -wave radiation pattern. Thus, correction of AVO amplitudes for radiation pattern performed under the assumption of the isotropic overburden is usually sufficient. Further, numerical tests show negligible influence of the free surface on AVO amplitudes for most cases. The factor that due to anisotropy most distorts AVO amplitudes in the overburden is geometrical spreading, which reflects the focusing and defocusing of energy. The distortion is significant especially for an overburden characterized by a high difference of Thomsen's parameters $\epsilon - \delta$ (≥ 0.15).

INTRODUCTION

Amplitude-variation-with-offset (AVO) analysis plays an important role in seismic exploration. Information contained in the amplitudes of seismic waves reflected from a target structure can be used for parameter estimates of the reservoir. The complexity of AVO responses, however, causes many difficulties in AVO analysis, so results can be easily misinterpreted. Thus, the reliability of AVO analysis is still in question.

Since hydrocarbon reservoirs and the overlying medium itself often are anisotropic, it can be important to take that anisotropy into account in computing reflection coefficients in AVO analysis. Both isotropic and anisotropic reflection/transmission (R/T) coefficients have been treated in the past, for example, by Aki & Richards (1980), Červený *et al.* (1977), and Daley and Hron (1977). In practice, approximations of R/T coefficients play an important role in AVO analyses. Such approximations can be found, for instance, in Banik (1987), Thomsen (1993), and most recently in Rüger (1997, 1998).

In order to make any parameter estimates of a hydrocarbon reservoir, reflection coefficients from the reservoir layer have to be extracted from AVO amplitudes, or equivalently, AVO amplitudes have to be “corrected” for propagation phenomena associated with the overburden. In most cases, a raw AVO response is corrected for geometrical spreading (Ursin, 1990; Castagna, 1993) and radiation pattern (Krail and Shin, 1990; Castagna, 1993), both computed for a homogeneous isotropic layer (or a stack of horizontal layers). Other phenomena, however, may also distort AVO responses. The radiation pattern of a source located close to a structural interface such as the Earth’s surface or a borehole wall may differ significantly from the radiation pattern in a homogeneous layer. Also, the wavefield recorded at or close to a structural interface is influenced by its presence; geophones located on Earth’s surface is a typical example. Transmission losses due to a finely-layered overburden may cause strong distortions of AVO amplitudes. Martinez (1993) has also discussed the non-negligible influence on AVO of attenuation, as well as of multiples and $P - SV$ converted modes.

Conventional amplitude corrections are adequate if the components of the propagation factor (discussed later on) change slowly with offset. This assumption seems to be reasonable for small offset-to-depth ratio and “smooth” isotropic overburden (elastic parameters of a “smooth” medium do not change significantly over the distance corresponding to the predominant wavelength). Propagation phenomena in a layered isotropic overburden have been discussed in the past, for example, by Martinez (1993). However, the AVO corrections based on the assumption of the isotropic wave propagation can break down if the overburden is anisotropic.

For our purpose it is useful to separate the AVO response into two parts: a) the reflection coefficient from the target and b) the *propagation factor*, which I define as the product of the radiation pattern of the source, geometrical spreading, transmission coefficients along the raypath and free-surface coefficient (the coefficient describing the influence of the Earth’s surface). As is true for the reflection coefficient, the

propagation factor is a function of offset. Thus, for AVO analysis to be successful in extracting angle-dependent reflection coefficients, it is important to correct for the propagation factor in the AVO response.

Here, I study the anisotropic propagation factor by modeling AVO responses for a simple VTI shale model introduced by Kim *et al.* (1993). The results show that even for such a simple model, AVO analysis cannot be carried out without taking propagation phenomena into account.

NUMERICAL MODELING

MODEL

I examine the influence of an anisotropic overburden for a modified version of the model originally introduced by Kim *et al.* (1993), which can be considered as representative of a sedimentary shale/sand formation. The model used in this paper (Figure 1) consists of three homogeneous layers: isotropic near-surface layer, VTI shale layer and isotropic gas-sand layer. The “reflector” (top of the sand layer) is characterized by a strong positive normal-incidence P -wave reflection coefficient; its depth (2.6 km) is fixed in all computations below. The thickness of the near-surface layer z is kept at 500 m, unless specified differently.

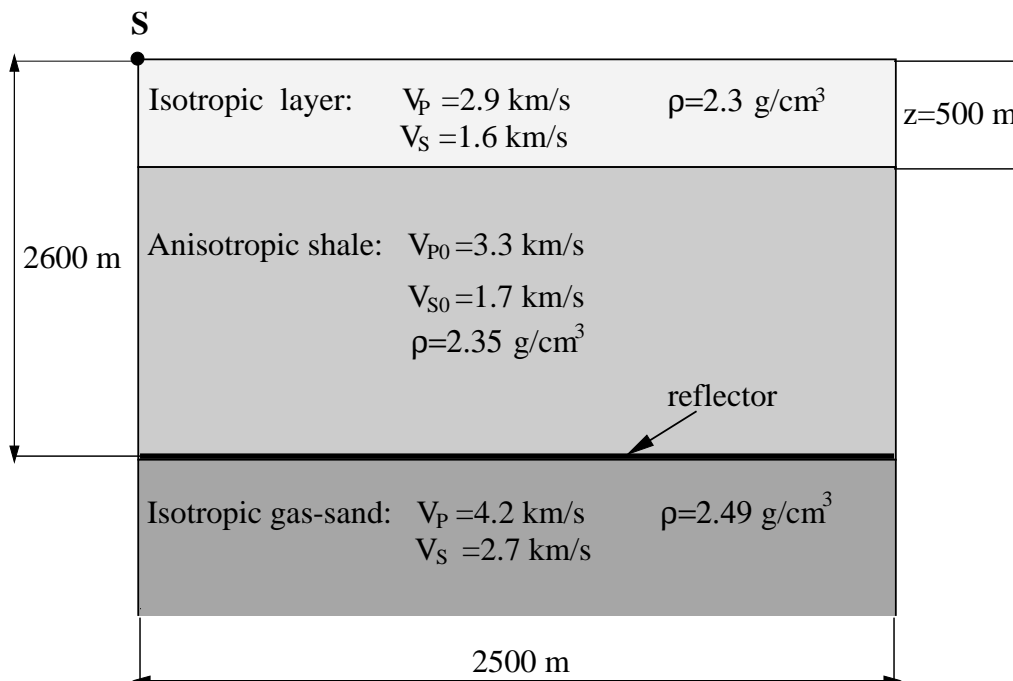


FIG. 1. Anisotropic model used in this work: the parameters of the shale layer are as follows: MT (Model Typical): $\delta = 0.1, \epsilon = 0.2$; MS (Model Strong): $\delta = -0.22, \epsilon = 0.195$; ME (Model Elliptical): $\delta = \epsilon = 0.13$.

Three different pairs of the anisotropic coefficients of the shale layer are considered. Following Thomsen's (1986) notation, I introduce three models: a) MT (**T**ypical) is characterized by typical values for shales $\delta = 0.1, \epsilon = 0.2$ (Tsvankin, 1995); b) MS (**S**trong) has $\delta = -0.22, \epsilon = 0.195$ (the anisotropy is strong in terms of the large difference $\epsilon - \delta = 0.415$); and c) ME (**E**lliptical) has elliptical anisotropy with $\delta = \epsilon = 0.13$.

AVO RESPONSES

I performed computations for a vertical single force (Ricker wavelet with a dominant frequency of 25 Hz) and 50 receivers located on the free surface at offsets 50 - 2500 m (giving a maximum offset-to-depth ratio of 0.96). All AVO responses computed in this paper represent pure P -modes reflected from the shale/sand interface (absolute amplitudes).

In the following, different components of the propagation factor (radiation pattern, free-surface coefficients, transmission coefficients and geometrical spreading) are analyzed in order to investigate their individual influence on the AVO amplitudes.

“Full” AVO amplitudes and reflection coefficients.—

Figure 2 shows “full” reflection amplitudes (left-hand side) computed for the model introduced in Figure 1 and the corresponding P -wave reflection coefficients (right-hand side). For comparison, plots are supplemented by thin solid curves labeled “ISO” computed for the purely isotropic model ($\epsilon = \delta = 0$ in the shale layer). Since offsets up to 2500 m represent a pre-critical region, all plotted quantities are real; that is, the phase shift is zero. Full AVO amplitudes simulate amplitudes in the data collected on the free surface, while the reflection coefficient is the quantity one wants to extract from the data. The propagation factor is responsible for the difference between the full AVO amplitudes and reflection coefficients.

Figure 2 shows two basic differences between AVO and reflection responses. First, the AVO curves differ at small offsets for different anisotropic models, whereas the reflection coefficients for the same offsets are close to each other (which one would expect, since anisotropy of VTI medium has no influence on normal-incidence reflection and transmission coefficients). The fact that the AVO amplitudes are different for normal-incidence reflections in a VTI medium may seem surprising. The differences are due to the focusing of energy during propagation through the anisotropic overburden for different models (Tsvankin, 1995). This phenomenon will be discussed below in more detail. Second, the anisotropic overburden distorts the AVO gradient, a crucial quantity in AVO analysis. From Figure 2, it is clear that a correction of AVO amplitudes for propagation through anisotropic overburden is necessary in AVO analyses.

Interestingly, the reflection coefficients computed as functions of offset (Figure 2) almost coincide for all models (both isotropic and anisotropic), whereas the same re-

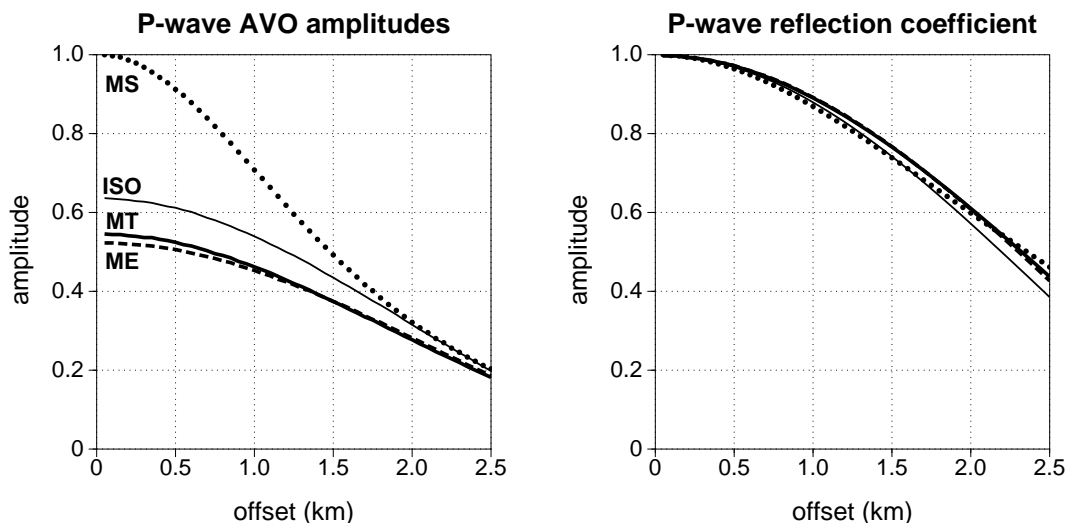


FIG. 2. Full AVO amplitudes computed for different parameters of the shale layer (left) and the corresponding P -wave reflection coefficients (right) as functions of offset. The solid, dotted and dashed curves represent MT, MS and ME models, respectively. The thin solid curve is computed for the isotropic model. AVO amplitudes are normalized by the factor $0.66E - 3$, the amplitude at zero-offset for the MS model; the reflection coefficients by the factor 0.148, which is the true zero-offset reflection coefficient.

Reflection coefficients recomputed as functions of incidence phase angle at the shale/sand interface have distinctly different AVO gradients (Figure 3). For a fixed offset, different anisotropic models yield different incidence phase angles at the reflector due to the splitting of phase and group velocity vectors in the overburden. For example, offset 2.5 km corresponds to an incidence phase angle of 29° for model MS but only 22° for model MT (see Figures 2 and 3). Thus, the computation of reflection coefficient as a function of incidence phase angle has to take into account the anisotropy along the raypath in order to obtain the AVO gradient suitable for parameter estimation.

Unfortunately, such a recomputation can be difficult in practice because it requires knowledge of the medium parameters. Moreover, in anisotropic media without a horizontal symmetry plane, the incidence group angle (the angle between the ray and the normal to the interface) may differ from the group angle of reflection even for the pure P -mode. Also, the incident and reflected rays can lie in different vertical planes, which may significantly complicate the recovery of the incidence angle at the reflector. The distortion of the whole raypath (from that in isotropic medium) and the splitting of group- and phase-velocity vectors due to anisotropy are main reasons why ignoring anisotropy in the overburden can lead to erroneous interpretation.

Radiation pattern.—

The radiation pattern of a seismic source is controlled by three factors: a) geome-

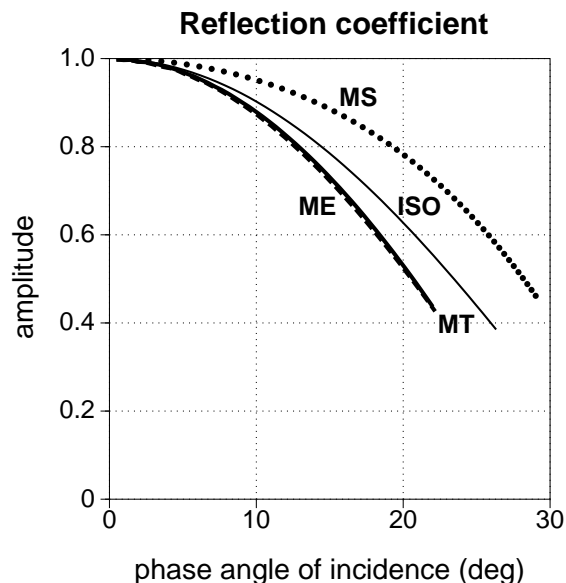


FIG. 3. Reflection coefficients as functions of phase angle recomputed from Figure 2. The curves represent different anisotropic parameters of the shale in accordance with the convention used in Figure 2. Reflection coefficients are again normalized by the factor 0.148.

try of the source, b) the existence of a structural interface in the vicinity of the source and c) parameters of the medium surrounding the source.

The geometry of the source (e.g., it may be a point single force or an explosion) imposes a generally well-known shape on the radiation pattern (Aki & Richards, 1980). While AVO responses are commonly corrected for this geometrical factor, the other two above factors are frequently ignored in AVO analyses, partly also because the information needed for such corrections may not be available. However, sources are often located at or close to Earth's surface, a borehole wall or subsurface layer boundaries. The existence of a nearby interface can make the radiation pattern frequency dependent (Jílek and Červený, 1996). Finally, anisotropy of the medium surrounding the source influences its radiation pattern as well. This will be discussed at the end of this section.

In the absence of nearby interfaces, the P -wave radiation pattern of a vertical single force in an isotropic or VTI layer (the source used in this paper) as a function of radiation angle is given by

$$R_P(\alpha) = \frac{F_P(\alpha)}{4\pi\rho V_{P0}^2}, \quad (1)$$

where α is the radiation angle (the angle with vertical of the ray connecting the source and receiver), ρ is density and V_{P0} is the vertical P -wave velocity. $F_P(\alpha)$ is the projection of the force onto the P -wave polarization vector. For a source located

within an isotropic layer, the polarization vector coincides with the direction of the ray. Then, $F_P(\alpha)$ and the radiation pattern as a whole are proportional to $\cos \alpha$. The radiation pattern defined by expression (1) is contained in the equation for P -wave amplitudes in a VTI layer derived by Tsvankin (1995). That definition is also in agreement with the so-called “ray-theory radiation pattern” presented, for instance, in Jílek and Červený (1996).

Equation (1) does not account for either the Earth’s surface or any other structural interface in the vicinity of the source. However, Jílek and Červený (1996) showed that for a vertical single force located on the Earth’s surface, the P -wave radiation pattern is almost the same as in full space (e.g., the radiation pattern is proportional to $\cos \alpha$). Thus, equation (1) is sufficiently accurate for the purpose of this paper and may be acceptable in the presence of the Earth’s surface.

In Figure 4, the radiation pattern is plotted as a function of offset for the purely isotropic model from Figure 1. The radiation pattern varies by about 8% within the range of offsets from 0 to 2.5 km (corresponding to a maximum radiation angle of 23°), which is a relatively small, but not negligible, variation. Figure 4 suggests that, in general, AVO amplitudes should be corrected for the radiation pattern. The influence of the radiation pattern on AVO response would be even more pronounced for larger offset-to-depth ratios or in the case of a high-velocity near-surface layer.

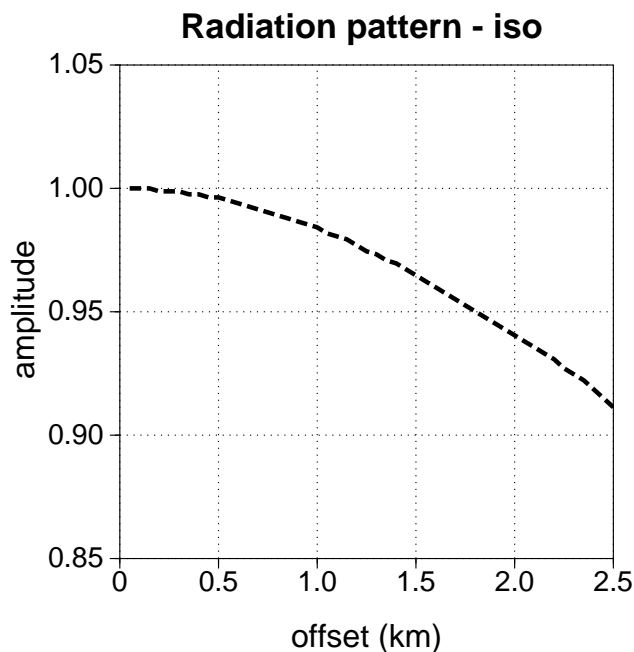


FIG. 4. Radiation pattern of a vertical single force as a function of offset computed for the purely isotropic model from Figure 1. The amplitude is normalized by 0.008 to give unity at zero offset.

Figure 5 shows the influence of anisotropy in the VTI shale layer on the radiation

pattern (the near-surface layer remains isotropic; see Figure 1). Figure 5 represents the departure of the radiation pattern from that in Figure 4. Comparison with Figure 4 shows that radiation patterns differ somewhat for different anisotropic models despite the fact that the source is located within the isotropic layer. The reason for any difference is, again, the splitting of phase- and group-velocity vectors due to anisotropy along the ray connecting a certain source-receiver pair. Figure 5, however, also shows that the influence of anisotropy on the radiation pattern does not exceed $\pm 3\%$, a negligible distortion in terms of AVO amplitudes. For typical sand/shale formations, anisotropy of the overburden is not strong enough to cause deviations in the radiation angle (from the isotropic value) that are large enough to result in a measurable distortion of the radiation pattern. Thus, as an important result, corrections of AVO amplitudes for radiation pattern in shale/sand formations can ignore anisotropy of the overburden.

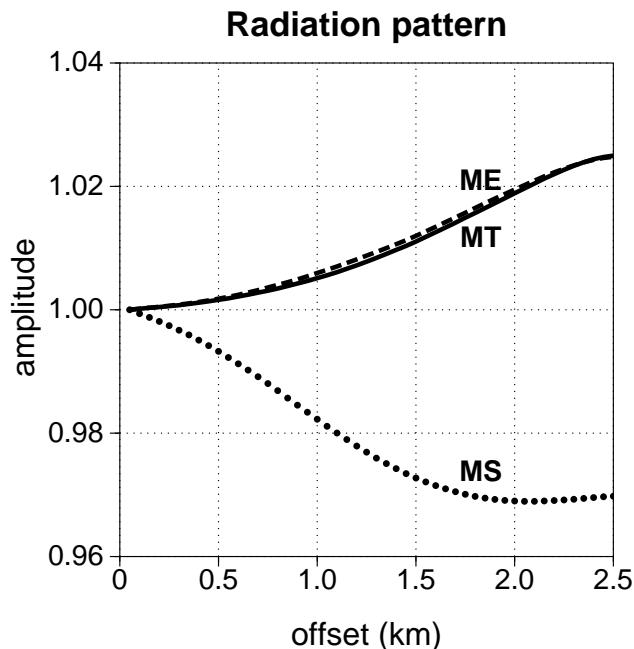


FIG. 5. Radiation pattern of a vertical single force as a function of offset computed for models MT (solid curve), ME (dashed curve) and MS (dotted curve). The curves are normalized by the curve from Figure 4 computed for the purely isotropic model.

Finally, what happens if the near-surface layer that contains the source is anisotropic as well? In this case, equation (1) is still valid, while the polarization vector no longer coincides with the direction of the ray (or group velocity vector). However, Tsvankin and Chesnokov (1990) showed that, typically, P -wave group velocity and polarization vectors lie close to each other, with the deviation less than $\pm 2^\circ$. Then, the resulting error in the radiation pattern does not exceed 4% for radiation angles up to 45° . Anisotropy in the source layer, however, contributes to distortions of geometrical

spreading factor due to energy focusing, as discussed below.

Free-surface coefficients.—

The free-surface coefficient is another quantity contained in the propagation factor. Receivers located on the Earth's surface record an interference wavefield that contains not only the direct P -wave approaching the surface but also PP and PS reflections from the Earth's surface. Such a superposition of the three arrivals can be characterized by a quantity called the *free-surface* coefficient. In the literature, this quantity is also sometimes called the *conversion* coefficient (see, for example, Červený *et al.*, 1977). Conventionally, the free-surface coefficient is ignored in AVO corrections.

The free-surface coefficient depends on the incidence angle of the direct P -wave at the Earth's surface. In Figure 6, the free-surface coefficients for the three models (MT, ME and MS) are plotted as functions of offset. The offset of 2.5 km is related to the incidence angles 19° and 26° for models MT and MS, respectively (for model ME, the incidence angle is practically the same as for model MT).

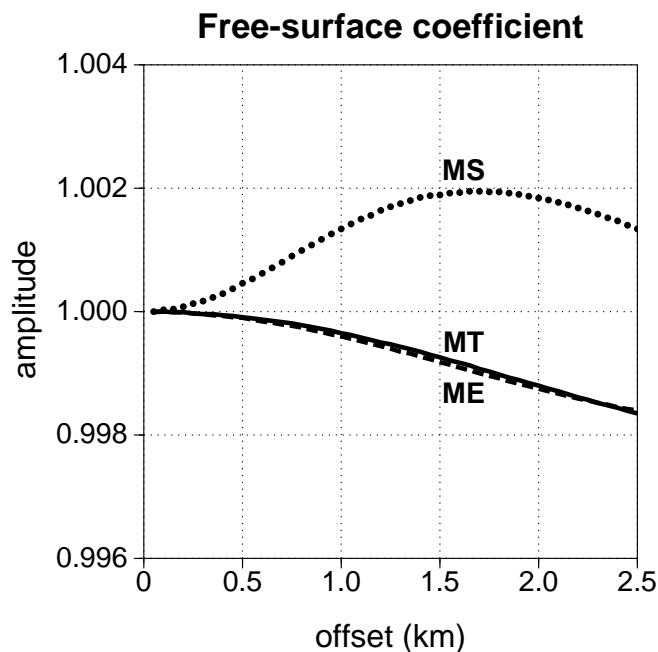


FIG. 6. Free-surface coefficients as functions of offset computed for models MT, ME and MS ($V_P/V_S = 1.8$ in the near-surface isotropic layer). The coefficients are normalized by the corresponding values for the isotropic model.

The results for free-surface coefficients are similar to those for the radiation patterns. Splitting of phase- and group-velocity vectors in the VTI layer leads to different responses for the three models, despite the fact that near-surface layer is isotropic.

The influence of anisotropy, however, is even smaller than that for the radiation pattern (no more than 0.5% of the isotropic free-surface coefficient). Hence, the anisotropy of the overburden can be safely ignored in the computation of the free-surface coefficients.

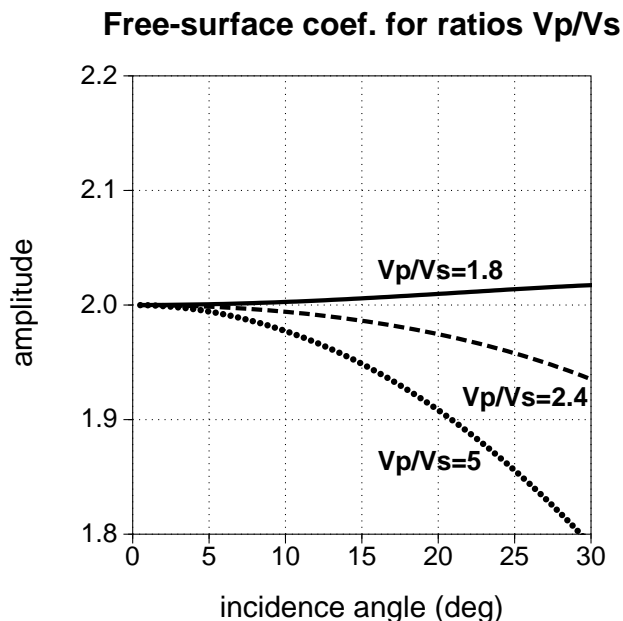


FIG. 7. Free-surface coefficient as a function of the incidence angle at the Earth's surface computed for three ratios V_P/V_S of the isotropic near-surface layer (for offset-to-depth ratio up to unity, incidence angles do not usually exceed 30°). The solid curve corresponds to $V_P/V_S = 1.8$ (the ratio used in models MT, ME and MS), the dashed and dotted curves to $V_P/V_S = 2.4$ and $V_P/V_S = 5$.

The angular dependence of the free-surface coefficient depends on the ratio V_P/V_S of the P - and S -wave velocities in the near-surface layer (Černý *et al.*, 1977). In Figure 7, the free-surface coefficients are plotted for three different V_P/V_S ratios for the isotropic near-surface layer. Clearly, for large ratios V_P/V_S and high incidence angles, the free-surface coefficients can change the angle dependence of the AVO amplitudes significantly. The departure from the behavior for isotropic models due to anisotropy, however, remain small, much as shown in Figure 6. Still, if the V_P/V_S ratio does not exceed 2.4 and the incidence angle does not exceed 35° , the variation of the total free-surface coefficients is less than 5%. Thus, the free-surface coefficients can be entirely ignored in AVO corrections for such cases. This conclusion is still valid if the near-surface layer is anisotropic, with parameters typical for shales.

Transmission coefficients.—

In general, the transmission coefficients along the raypath influence the recorded wavefields and should not be ignored in AVO corrections. Transmission coefficients

are defined as the ratio of the amplitudes of the transmitted and incident plane waves at an interface. Figure 8 shows the transmission coefficients as functions of offset for the interface between the isotropic and the VTI layers in Figure 1. The plot on the left-hand side shows the transmission coefficient for a P -wave propagating from the isotropic near-surface layer into the VTI layer (down), while the coefficients for the opposite propagation direction (up) are plotted on the right-hand side. For a given offset, the plots show the coefficients along the same raypath connecting the source and receiver.

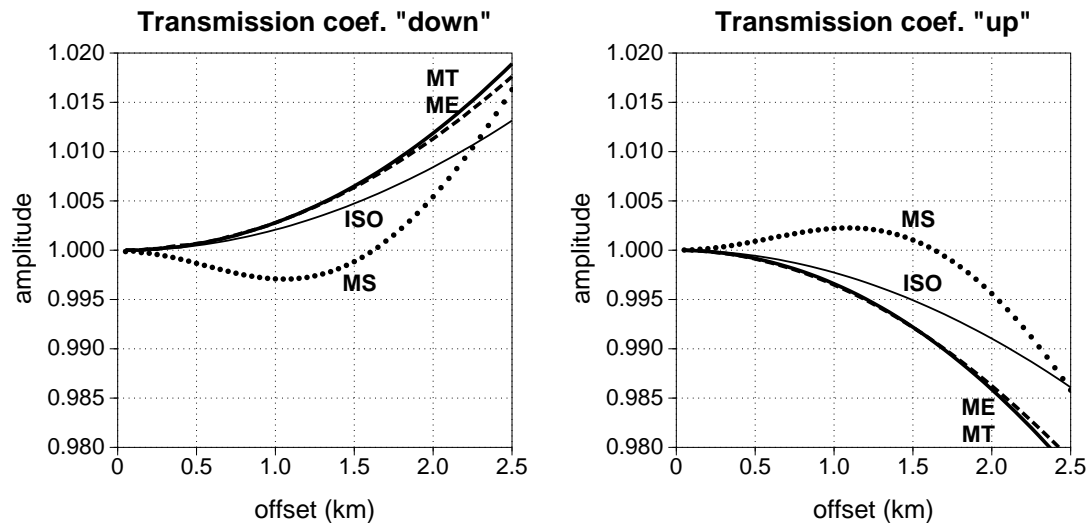


FIG. 8. Transmission coefficients for downgoing (left) and upgoing (right) waves at the top of the shale layer, as functions of offset. Curves are plotted according to the convention in Figure 2. The amplitudes are normalized by the factors 0.925 (down) and 1.075 (up), the transmission coefficients at zero-offset.

Note that the transmission coefficients on the way “down” and “up” are nearly “symmetric” in that their product for a given offset is close to unity. This is no surprise since two-way transmission coefficients across an interface are always close to unity unless the reflection coefficient is unusually large.

Transmission related to a single interface with a small velocity contrast are thus negligible in AVO analysis whether the layers are isotropic or anisotropic (for typical anisotropy of shales). Also, if the isotropic/shale interface in the model from Figure 1 is not strictly horizontal but exhibits some dip (up to approximately $\pm 20^\circ$), distortions of the AVO amplitudes caused by transmission coefficients remain negligible.

Unfortunately, a single isolated interface is not a common case in practice. The overburden usually consists of a large number of thin layers. The angle-dependent transmission losses due to fine layering can be large and differ in character from that shown here; multiples within the layered structure play an important role in the AVO response, and transmission losses are frequency dependent. These phenomena, however, are not treated in this paper.

Geometrical spreading.—

Geometrical spreading which characterizes the spatial distribution of energy density as the wave propagates away from the source, is an essential part of the propagation factor. Although the energy density usually decreases with the distance from the source, a local increase is also possible. For a homogeneous isotropic layer, amplitudes of seismic waves are proportional to the familiar spherical spreading factor $G(r)$ given by

$$G(r) = \frac{1}{r},$$

where r is the distance between the source and the receiver. In an anisotropic layer, the geometrical spreading depends not only on the distance r but also on the direction of the wave propagation. Tsvankin (1995) discussed the geometrical spreading for homogeneous transversely isotropic media. For weak transverse isotropy, he derived the P -wave spreading factor as

$$G(r, \theta) = \frac{1}{r} \frac{1 - 2(\epsilon - \delta) \sin^2 2\theta + \delta \sin^2 \theta}{1 + 2\delta}, \quad (2)$$

where θ is the phase angle, and δ and ϵ are Thomsen's (1986) anisotropy parameters.

It turns out that the geometrical spreading is the most important quantity influencing the offset dependence of the propagation factor. In the following, the geometrical spreading is computed for models MT, ME and MS and different thicknesses of the near-surface layer z (Figure 1).

Figure 9 shows geometrical spreading computed for $z = 0$, which corresponds to the single VTI layer (the case discussed in Tsvankin, 1995). For comparison, the figure is supplemented by the geometrical spreading curve labeled "MT2". Similarly to model MT, MT2 represents another typical anisotropic model characterized, however, by $\epsilon - \delta = 0.2$ for the shale layer. The curves are normalized by the geometrical spreading factor computed for the isotropic model ($G = \frac{1}{r}$ in that case). Compared to that of the other propagation quantities discussed above, anisotropy causes more substantial distortions in the geometrical spreading. Geometrical spreading is the only quantity in the propagation factor that gives rise to the differences in the full AVO amplitudes for small offsets between models MT MS, and ME in Figure 2. The anisotropic geometrical spreading at zero offset is governed by the parameter δ (see equation (2) for $\theta = 0$).

Using equation (2) and numerical modeling, Tsvankin (1995) showed that the important quantity contained in the anisotropic geometrical spreading is the difference $\epsilon - \delta$, rather than ϵ and δ themselves. This difference is largely responsible for focusing and defocusing of the energy along the wavefront. For a typical VTI shale layer with $\epsilon - \delta > 0$, the energy is concentrated near the vertical, and the energy flux decreases away from the vertical, with its minimum often close to 45° (for reference here, the offset of 2.5 km is related to a maximum angle of 26° for model MS).

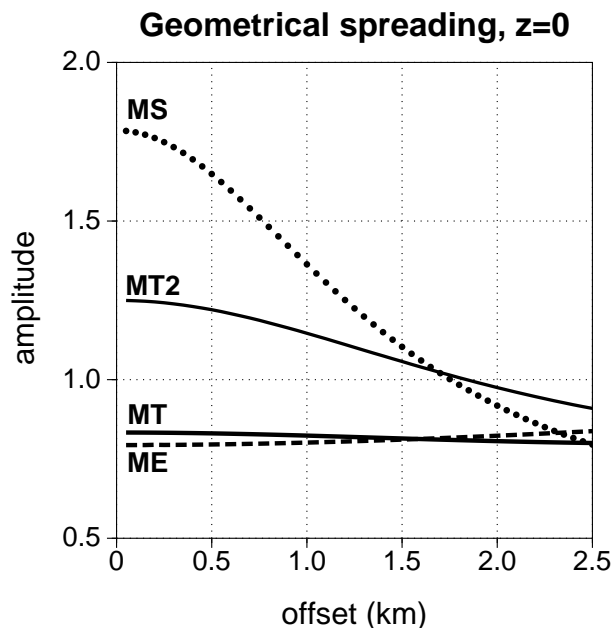


FIG. 9. The geometrical-spreading factor as a function of offset computed for zero thickness z of the near-surface layer. Curves are plotted for models MT, ME, MS and MT2. Model MT2, used by Tsvankin (1995), has $\delta = -0.1$ and $\epsilon = 0.1$ in the shale layer.

The focusing of energy is caused by a high concentration of rays close to the vertical. Figure 10 shows rays computed for models MT ($\epsilon - \delta = 0.1$, left) and MS ($\epsilon - \delta = 0.415$, right). The increment in the phase angle is constant (0.45°). The larger the difference $\epsilon - \delta$, the higher is the ray concentration close to the vertical and, consequently, the faster is the decrease in the amplitudes with offset (Figure 9). Note that for model MS ($\epsilon - \delta = 0.415$) the decrease in geometrical spreading due to anisotropy reaches 55% at 2.5 km. Also, for the typical shale anisotropy introduced in model MT2 ($\epsilon - \delta = 0.2$), the decrease reaches a significant value of 27%. On the other hand, for model ME, where $\epsilon - \delta = 0$, a slight increase in the anisotropic geometrical spreading factor is observed, which results in a small reduction in the amplitude decay with offset. For VTI media with $\epsilon - \delta < 0$, focusing of energy can lead to an unusual increase of the geometrical spreading factor and, consequently, AVO amplitudes with offset. Negative $\epsilon - \delta$, however, is not observed in typical shale/sand formations (Tsvankin, 1995).

In Figure 11a, the geometrical spreading for model MT is computed for different thicknesses of the subsurface isotropic layer z . Two general trends can be observed: the curves are shifted in the vertical direction, and they have different shapes. However, for model MT, such changes are quite mild. Notice that the limits $z \rightarrow 0$ and $z \rightarrow 2600$ m correspond to homogeneous anisotropic and homogeneous isotropic single-layer overburden, respectively. Thus, especially for small thicknesses z , anisotropy

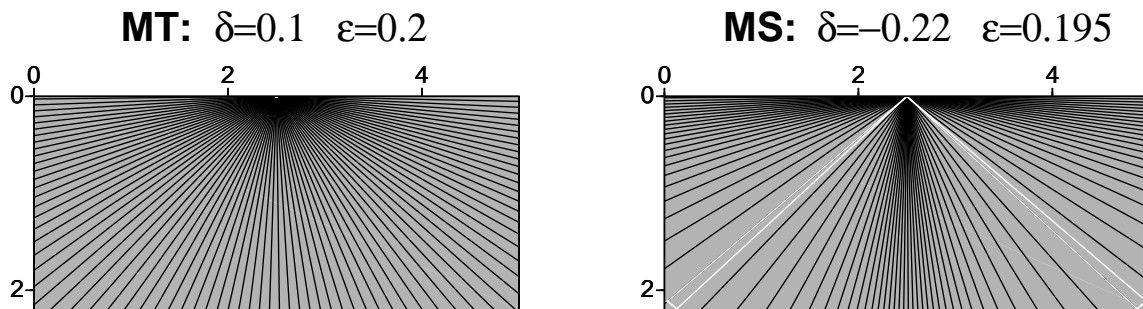


FIG. 10. Concentration of rays for models MT ($\epsilon - \delta = 0.1$, left) and MS ($\epsilon - \delta = 0.415$, right). The rays are computed for a constant increment in the phase angle. A high concentration of rays corresponds to high amplitude, and vice versa.

of the shale layer may cause non-negligible distortions. For instance, anisotropy in model MT changes the geometrical spreading by about 8% at an offset of 2.5 km for $z = 500$ m, see Figure 11a.

The variation in the geometrical spreading for different z is well pronounced in Figure 11b computed for model MS. If the overburden contains an anisotropic layer characterized by a relatively large $\epsilon - \delta$, the geometrical spreading is quite sensitive to the overburden structure.

Finally, Figure 12 shows the influence of anisotropy in the near-surface layer on the geometrical spreading. Figure 12 corresponds to models MT (12a) and MS (12b) as introduced in Figure 1 ($z = 500$ m), but the near-surface isotropic layer in both models is replaced with three different VTI layers. Both the vertical shift and the different shapes of the curves are observed again, although they differ from those in Figure 11.

Figures 11 and 12 illustrate a complex behavior of anisotropic geometrical spreading. Numerical tests show that the distribution of anisotropy within the overburden has an important influence on the shape of the geometrical spreading curve (i.e., the focusing of energy). Hence, in a horizontally layered overburden, spreading is determined not only by parameters of the individual layers but also their relative thicknesses. This fact may considerably complicate quantitative estimates of the geometrical-spreading correction.

SUMMARY

In general, anisotropy may cause non-negligible distortions of AVO amplitudes. Hence, the isotropic corrections of AVO responses may not be sufficient if the overburden is partly anisotropic.

Two phenomena observed in an anisotropic overburden do not exist in isotropic

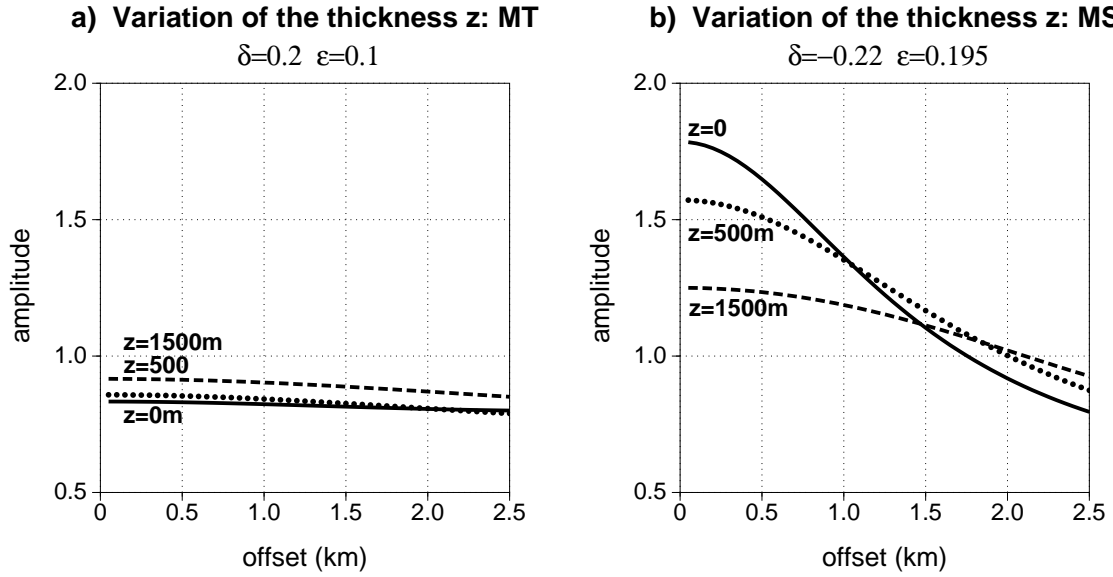


FIG. 11. Geometrical spreading factor for models a) MT and b) MS computed for different thicknesses z of the subsurface layer: solid curve - $z = 0$, dotted - $z = 500$ m, dashed - $z = 1500$ m. Each curve is normalized by the geometrical spreading factor computed for the corresponding isotropic model.

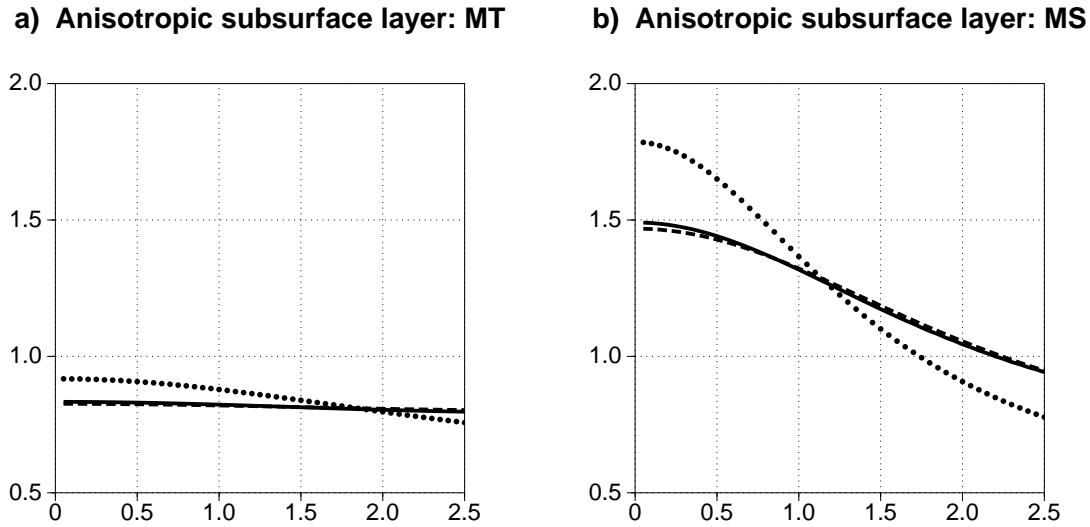


FIG. 12. Geometrical spreading for models a) MT and b) MS computed for three sets of anisotropic parameters of the near-surface layer ($z = 500$ m): solid curve - $\delta = 0.1, \epsilon = 0.2$, dotted - $\delta = -0.22, \epsilon = 0.195$, dashed - $\delta = \epsilon = 0.13$ (solid and dashed curves practically coincide). The curves are normalized by the geometrical spreading computed for the corresponding isotropic model.

media: focusing and defocusing of energy along the wavefront and splitting of phase and group velocity vectors. The focusing of energy influences geometrical spreading and, consequently, the AVO intercept and gradient. The splitting of phase and group velocity vectors within an anisotropic layer complicates AVO analysis since it changes the relationship between offset and the corresponding incidence angle at the reflector, the quantity governing angle-dependent reflection coefficients.

The radiation pattern is a quantity that should not be ignored in AVO correction. For typical shale/sand formations, however, the correction for the radiation pattern can be carried out without concern for anisotropy in the overburden. Except for large radiation angles (e.g., greater than 40°), such a correction is sufficiently accurate.

The influence of the Earth's surface on AVO amplitudes can be ignored for most cases, as long as both the ratio V_P/V_S in the near-surface layer and the incidence angle at the Earth's surface are within a reasonable range (approximately, the influence is negligible for V_P/V_S up to 2.4 and the incidence angles less than 35° for tested models). Angle-dependent transmission losses, which are insignificant for the two-layer overburden considered here, may be large for realistic multilayer models. This is a subject for future study.

Geometrical spreading is the main factor distorting the AVO gradient. Anisotropy of the overburden may have a strong influence on the geometrical spreading, a consequence of the focusing and defocusing of energy within the anisotropic medium. Thus, the correction of AVO amplitudes for geometrical spreading has to include possible anisotropy of the overburden, especially if the anisotropic layers are characterized by relatively large values of $\epsilon - \delta$ and small or negative δ . In general, geometrical spreading in a layered anisotropic overburden exhibits a complex behavior that depends on both the spatial distribution of the elastic parameters and the relative thicknesses of all layers. The correction of AVO amplitudes for the geometrical spreading should be supported by numerical modeling.

REFERENCES

- Aki, K., & Richards, P.G., 1980, Quantitative Seismology; theory and methods, vol.1: W.N.Freeman & Co., San Francisco.
- Banik, N.C., 1987, An effective anisotropy parameter in transversely isotropic media: Geophysics, **52**(12), 1654-1664.
- Castagna, J. P., 1993, AVO analysis - Tutorial and Review: *in* Offset dependent reflectivity, Castagna and Backus, Eds., SEG, Tulsa, 3-36.
- Červený, V., Molotkov, I. A., and Pšenčík, I., 1977, Ray method in seismology: Universita Karlova, Praha.
- Daley, P. F., & Hron, F., 1977, Reflection and transmission coefficients for transversely isotropic solids: Bull. Seis. Soc. Am., **67**, 661-675.
- Jílek, P., and Červený, V., 1996, Radiation patterns of point sources situated close to structural interfaces and to the earth's surface: PAGEOPH, Vol. 148, 175-225.

- Kim, K. Y., Wroldstad, K. H., & Aminzadeh, F., 1993, Effects on transverse isotropy on P-wave AVO for gas sands: *Geophysics*, **58** (6), 883-888.
- Krail, P. M., and Shin, Y., 1990, Deconvolution of a directional marine source: *Geophysics*, **55** (12), 1542-1548.
- Martinez, R. D., 1993, Wave propagation effects on amplitude variation with offset measurements: A modeling study: *Geophysics*, **58** (4), 534-543.
- Rüger, A., 1997, *P*-wave reflection coefficients for transversely isotropic models with vertical and horizontal axis of symmetry: *Geophysics*, **62**, 713-722.
- Rüger, A., 1998, Variation of *P*-wave reflectivity with offset and azimuth in anisotropic media: *Geophysics*, **63** (3), 935-947.
- Thomsen, L., 1986, Weak elastic anisotropy: *Geophysics*, **51** (10), 1954-1966.
- Thomsen, L., 1993, Weak anisotropic reflections: *in* Offset dependent reflectivity, Castagna and Backus, Eds., SEG, Tulsa, 103-111..
- Tsvankin, I. D., 1995, Body-wave radiation patterns and AVO in transversely isotropic media: *Geophysics*, **60** (5), 1409-1425.
- Tsvankin, I. D., and Chesnokov, E. M., 1990, Synthesis of body wave seismograms from point sources in anisotropic media: *Journal of Geophysical Research*, **95** (B7), 11317-11331.
- Ursin, B., 1990, Offset-dependent geometrical spreading in a layered medium: *Geophysics*, **55**, 492-496.